

# A Role for Thrombin Receptor Signaling in Endothelial Cells During Embryonic Development

Courtney T. Griffin,\* Yoga Srinivasan,\* Yao-Wu Zheng, Wei Huang, Shaun R. Coughlin†

The coagulation protease thrombin triggers fibrin formation, platelet activation, and other cellular responses at sites of tissue injury. We report a role for PAR1, a protease-activated G protein-coupled receptor for thrombin, in embryonic development. Approximately half of *Par1*<sup>-/-</sup> mouse embryos died at midgestation with bleeding from multiple sites. PAR1 is expressed in endothelial cells, and a PAR1 transgene driven by an endothelial-specific promoter prevented death of *Par1*<sup>-/-</sup> embryos. Our results suggest that the coagulation cascade and PAR1 modulate endothelial cell function in developing blood vessels and that thrombin's actions on endothelial cells—rather than on platelets, mesenchymal cells, or fibrinogen—contribute to vascular development and hemostasis in the mouse embryo.

The serine protease thrombin is the product of a highly regulated cascade of zymogen activation that is triggered when plasma coagulation factors meet tissue factor. Tissue factor is expressed by cells that do not directly contact blood and by cytokine-activated leukocytes and endothelial cells. In the adult, thrombin is generated in the setting of tissue injury or inflammation. Thrombin cleaves fibrinogen to fibrin monomer, which polymerizes to form fibrin matrices. Thrombin also activates platelets and endothelial cells. These observations and the phenotypes of gain-of-function and partial loss-of-function mutations in coagulation factor genes in humans cast the coagulation cascade and its effector protease thrombin in the role of orchestrating hemostatic and inflammatory responses to tissue injury (1–3).

Cellular responses to thrombin are mediated, at least in part, by protease-activated G protein-coupled receptors (PARs) (3). Mouse embryos lacking PAR1 or coagulation factors die with varying frequency at midgestation, often with signs of bleeding (4–10). We sought to define the cellular basis for death of *Par1*<sup>-/-</sup> embryos and the relation between the phenotypes caused by deficiencies in coagulation factors and PAR1.

Matings between *Par1*<sup>+/-</sup> and *Par1*<sup>-/-</sup> mice in a C57BL/6J background (≥97%) yielded 135 *Par1*<sup>+/-</sup> and 73 *Par1*<sup>-/-</sup> progeny (number of *Par1*<sup>-/-</sup> offspring was 54% of that expected by Mendelian inheritance;  $P < 0.001$  by chi-square test). Of the *Par1*<sup>-/-</sup> offspring, 36 were females, and 37 were males.

These results confirmed the partial embryonic lethality initially reported in mixed 50%C57BL/6J-50%129/Sv and in pure 129/Sv backgrounds (4, 11). *Par1*<sup>-/-</sup> × *Par1*<sup>-/-</sup> matings continued to yield approximately 50% embryonic loss over ~15 generations. This observation and the similar frequencies of embryonic death in the C57BL/6J and 129/Sv inbred backgrounds suggest that the partial penetrance of the *Par1*<sup>-/-</sup> phenotype is not due to a modifier gene.

Characterization of *Par1*<sup>-/-</sup> embryos in the C57BL/6J (≥97%) background revealed hemorrhage and cardiovascular failure at midgestation (12) (Fig. 1). At embryonic day 8.75 (E8.75), *Par1*<sup>-/-</sup> and wild-type embryos were indistinguishable by gross appearance, and somite counts were present in equal numbers in *Par1*<sup>+/-</sup> × *Par1*<sup>+/-</sup> litters. At E9.5, gross examination revealed blood in the exocoelomic and/or pericardial cavities in 22% of *Par1*<sup>-/-</sup> embryos. These embryos were pale, and their yolk sacs lacked blood-filled vessels. Embryos with gross bleeding usually had a dilated pericardial sac, a sign of cardiovascular failure. By E10.5, bleeding was seen in 35% of *Par1*<sup>-/-</sup> embryos; pericardial bleeding was especially prominent (Fig. 1D). By E12.5, 52% of *Par1*<sup>-/-</sup> embryos were dead with evident bleeding. The remaining E12.5 *Par1*<sup>-/-</sup> embryos were alive and appeared normal. Analysis of histological sections of gravid uterine segments containing *Par1*<sup>-/-</sup> embryos revealed that bleeding occurred earlier and more frequently than was apparent by gross examination (Fig. 1A). Collections of extravasated blood cells were seen as early as E9.0, before gross bleeding was detected, and by E9.5, blood cells were detected in the exocoelomic, amniotic, and/or pericardial and peritoneal cavities in 19 of 29 *Par1*<sup>-/-</sup> embryos (66%). No bleeding was detected in 16 wild-type E9.5 embryos exam-

17. R. L. Johnson, R. D. Riddle, E. Laufer, C. Tabin, *Biochem. Soc. Trans.* **22**, 569 (1994).
18. H. Roelink et al., *Cell* **81**, 445 (1995).
19. Phosphorothiolated *QSulf-1* antisense oligonucleotides (5'-CCAAGAGTCTCATAG-3', 5'-GAGCACTGCCAAGAAG-3', and 5'-CTCTTGCTGCACACGGC-3') were modified by phosphorothiolation of the first four and last four linkages and purified by high-performance liquid chromatography. Oligonucleotide pairs 1 and 2 and 1 and 3 inhibited *QSulf-1* mRNA accumulation in stage 12 embryos. Oligonucleotide pair 2 and 3 did not disrupt expression and served as a negative control along with a random oligonucleotide: 5'-CTATGGTACGATCAACG-3'. Embryos were cultured with antisense oligonucleotides as previously described (14).
20. A. G. Borycki et al., *Development* **126**, 4053 (1999).
21. S. Hoppler, J. D. Brown, R. T. Moon, *Genes Dev.* **10**, 2805 (1996).
22. S. Tajbakhsh et al., *Development* **125**, 4155 (1998).
23. E. Hirsinger et al., *Development* **124**, 4605 (1997).
24. F. Reichsman, L. Smith, S. Cumberledge, *J. Cell Biol.* **135**, 819 (1996).
25. M. Tsuda et al., *Nature* **400**, 276 (1999).
26. 10T1/2 cells were transfected with Eugene 6 (Boehringer/Mannheim) and transferred onto uncoated glass cover slips for 24 hours. Unpermeabilized cells were incubated for 1 hour at room temperature in a 1/500 dilution of 9E10 monoclonal antibody to myc or antibody to  $\beta$ -tubulin (Boehringer/Mannheim), washed, fixed in 2% paraformaldehyde, and incubated for 1 hour with 1/500 dilution of Cy3 anti-mouse antibody (Jackson Immuno Research) in the presence of 10% fetal bovine serum. Permeabilized cells cultured on cover slips were prefixed in 2% paraformaldehyde before primary and secondary antibody staining. For Western blot analysis, cell extracts and medium from transfected cultures were resolved by electrophoresis on SDS gels, transferred to nitrocellulose, and probed with 9E10 antibody to myc. Antibody staining was visualized with chemiluminescence (SuperSignal; Pierce Chemicals).
27. G. K. Dhoot et al., unpublished data.
28. G. Wei et al., *J. Biol. Chem.* **275**, 27733 (2000).
29. H. Shimizu et al., *Cell Growth Differ.* **8**, 1349 (1997).
30. Full-length *QSulf1* cDNA was cloned into the pAG-myc vector (*QSulf1-myc*). C2C12 myoblasts were transfected with expression plasmids with a calcium phosphate protocol. Stably transfected clones were selected with hygromycin. Individual and pooled (200) clones were assayed for *QSulf1* expression by immunostaining and Western blotting and for *Wnt1* signaling activity by cotransfection with TCF luciferase reporter genes and with Renilla control vector (Promega Dual Luciferase Reporter Assay System). After 6 hours, transfected cells were cocultured for 24 hours with *Wnt1*-expressing or control rat B1a cells, in the presence or absence of heparin (Sigma; porcine intestinal mucosal) or sodium chlorate (Sigma). For some studies, WT9 *QSulf1*-expressing C2C12 cells were retransfected with *QSulf1-myc* or mutant *QSulf1-myc* (CC89,90AA) plasmids, as a mixture pAG empty vector, in a total of 1.5  $\mu$ g of DNA per transfection.
31. F. Safaiyan et al., *J. Biol. Chem.* **274**, 36267 (1999).
32. K. Kamimura et al., *J. Biol. Chem.* **276**, 17014 (2001).
33. Single-letter abbreviations for the amino acid residues are as follows: A, Ala; C, Cys; D, Asp; E, Glu; F, Phe; G, Gly; H, His; I, Ile; K, Lys; L, Leu; M, Met; N, Asn; P, Pro; Q, Gln; R, Arg; S, Ser; T, Thr; V, Val; W, Trp; and Y, Tyr.
34. We thank M. Lai for excellent technical assistance; G. Esko, J. Raper, B. Vogelstein, and T. Brown for valuable reagents; and A.-G. Borycki and B. Brunk for helpful advice. We thank the NIH for a grant to C.P.E., the Royal Veterinary College for salary support to G.K.D. during sabbatical leave at the University of Pennsylvania School of Medicine, and the Royal Society and Wellcome Trust for ongoing research support to G.K.D.

9 April 2001; accepted 10 July 2001

Cardiovascular Research Institute, University of California at San Francisco (UCSF), San Francisco, California 94143

\*These authors contributed equally to this work.

†To whom correspondence should be addressed. E-mail: coughlin@cvrmail.ucsf.edu

REPORTS

ined in parallel. Of the 19 E9.5 *Par1*<sup>-/-</sup> embryos with microscopic bleeding, four had not developed dilated pericardial sacs or other apparent abnormalities, and live E9.5 to E10.5 embryos with both gross bleeding and vigorous heart beats were occasionally seen. Dead embryos always had evidence of bleeding. At face value, these observations suggest that bleeding preceded and probably caused rather than resulted from cardiovascular failure.

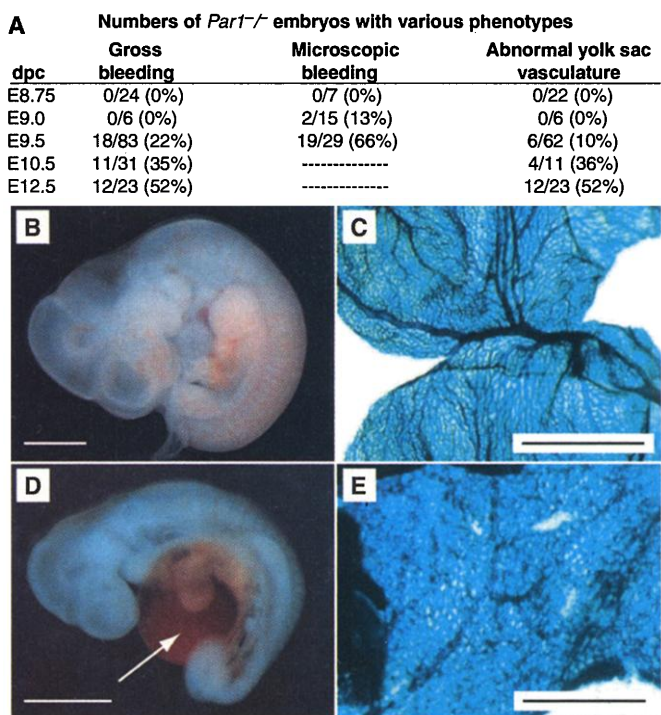
Why do *Par1*<sup>-/-</sup> embryos bleed? Blood in the exocoelomic and pericardial cavities of *Par1*<sup>-/-</sup> embryos implies bleeding from extraembryonic vessels and from the embryo proper, suggesting a general defect in hemostatic mechanisms or in the vasculature itself. It is unlikely that defective thrombin signaling in platelets accounts for bleeding in *Par1*<sup>-/-</sup> embryos because (i) *Par1*<sup>-/-</sup> platelets respond normally to thrombin (4), (ii) mice that do have platelets with defective thrombin signaling (13, 14) or that lack platelets (15) develop normally, and (iii) platelets are not present at E9.5 (16). PAR1 is highly expressed in endocardium and endothelium in E9.5 embryos by RNA in situ hybridization (17). However, other cell types in the embryo also express PAR1 (17), and fibroblasts cultured from mouse embryos express sufficient PAR1 to mediate thrombin signaling (4). To better characterize PAR1 expression, we generated PAR1-*LacZ* “knock-in” mice (18).  $\beta$ -Galactosidase staining of E9.5 PAR1-*LacZ* knock-in embryos (12, 18) revealed PAR1 expression in endocardium and vascular endothelium in great and small vessels, in occasional round cells adhering to the vessel wall, and in a subset of mesenchymal-appearing cells in the septum transversum and elsewhere (Fig. 2, A to D). Assessment of vascular and cardiac anatomy by light microscopy, whole-mount staining for platelet-endothelial cell adhesion molecule (PECAM-1) (Fig. 2, E and F), and  $\beta$ -galactosidase staining for a *LacZ* transgene driven by the endothelial-specific TIE2 promoter-enhancer (TIE2p/e-*LacZ*; see Fig. 1) (19) revealed variable developmental delay in *Par1*<sup>-/-</sup> embryos but no gross vascular malformation. Similarly, the fraction of cells positive for the endothelial marker intercellular cell-adhesion molecule-type 2 (ICAM2) by flow cytometry was not different between E9.5 *Par1*<sup>+/+</sup> and *Par1*<sup>-/-</sup> embryos, and transmission electron microscopy, immunostaining for smooth muscle  $\alpha$ -actin, and  $\beta$ -galactosidase staining for a smooth muscle  $\alpha$ -actin promoter-*LacZ* transgene did not reveal consistent differences. However, analysis of complete serial sections of three *Par1*<sup>-/-</sup> E9.5 embryos with hemopericardium did reveal a breach in the wall of the sinus venosus in two embryos (Fig. 2G). These openings appeared large enough to allow blood cells to enter the pericardial cavity from the intravascular space, and they were

unlikely to be artifacts of handling because similar defects were seen in serial sections of uterine segments containing E9.5 *Par1*<sup>-/-</sup> embryos embedded en bloc before sectioning. In the extraembryonic vasculature,  $\beta$ -galactosidase staining of yolk sacs from E8.5 *Par1*<sup>-/-</sup> embryos carrying the TIE2p/e-*LacZ* transgene revealed a normal-appearing primary vascular plexus. However, by E9.5, embryos with gross bleeding showed an abnormal yolk sac vascular pattern—usually delayed vascular remodeling (Fig. 1, A, C, and E). Yolk sac vascular abnormalities were seen only in embryos with gross bleeding, and it is possible that they were secondary to bleeding and cardiovascular collapse. However, the defects noted in the walls of great vessels in the embryo proper were almost certainly the source of, rather than the result of, bleeding. Taken together, these observations raised the possibility that loss of PAR1 signaling in endocardial and/or endothelial cells might be the primary defect in *Par1*<sup>-/-</sup> embryos and the direct or indirect cause of bleeding and death.

If loss of PAR1 function in endothelial cells were the primary defect in *Par1*<sup>-/-</sup> embryos, endothelial-specific expression of PAR1 should prevent death of *Par1*<sup>-/-</sup> embryos. To test this prediction, we generated transgenic mouse lines from two independent founders in which the endothelial-specific TIE2 promoter-enhancer (TIE2p/e) (19) drove mPAR1 expression (18). Transgene

expression could be detected as early as E8.0 by the reverse transcriptase-polymerase chain reaction (RT-PCR), and in situ hybridization of E9.5 and 13.5 embryos demonstrated selective expression of the transgene in endothelium and endocardium (Fig. 3A). Fibroblasts from *Par1*<sup>-/-</sup> mice bearing the transgene did not show thrombin-triggered increases in cytosolic calcium (Fig. 3B)—additional evidence for cell type-specific transgene expression. In crosses designed to yield equal numbers of transgenic and nontransgenic *Par1*<sup>-/-</sup> and *Par1*<sup>+/+</sup> mice, transgene-negative *Par1*<sup>-/-</sup> offspring were generated at approximately half the expected frequency, but transgene-positive *Par1*<sup>-/-</sup> pups were born at a frequency indistinguishable from *Par1* heterozygotes (Fig. 3C). Similar results were obtained using the transgenic line from an independent founder. To directly examine the effect of the transgene on *Par1*<sup>-/-</sup> embryos, *Par1*<sup>+/+</sup> mice hemizygous for the transgene were crossed with *Par1*<sup>-/-</sup> mice, and E11.5 to E12.5 embryos were scored as alive or dead and genotyped (Fig. 3D). The death rate associated with PAR1 deficiency was 39% in transgene-negative embryos but only 14% in transgene-positive embryos ( $P < 0.001$  by chi-square test). The live transgene-positive *Par1*<sup>-/-</sup> embryos appeared normal. Thus, in three separate experiments, the TIE2p/e-PAR1 transgene greatly reduced or prevented embryonic death due to

**Fig. 1.** Phenotype of *Par1*<sup>-/-</sup> embryos. (A) Frequency of abnormalities at various gestational ages (dpc, days post coitum). Gross bleeding indicates the presence of pooled blood in the pericardial or exocoelomic cavities detected with a dissecting microscope. Microscopic bleeding indicates the presence of collections of embryonic blood cells in the pericardial and/or peritoneal, amniotic, and/or exocoelomic cavity as detected in serial sections of gravid uterine segments embedded en bloc (i.e., minimally manipulated). Abnormal yolk sac vasculature indicates disorganization or delayed remodeling based on PECAM-1 immunostaining and TIE2p/e-*LacZ* staining at E8.75 to E10.5 and lack of blood-filled yolk sac vessels at E12.5.



(B and D) *Par1*<sup>+/+</sup> (B) and *Par1*<sup>-/-</sup> (D) littermate E10.5 embryos. Note developmental delay and dilated, blood-filled pericardial cavity (arrow) in the *Par1*<sup>-/-</sup> embryo. (C and E) Yolk sacs from the embryos shown in (B) and (D), respectively. These embryos carried a TIE2p/e-*LacZ* transgene to allow visualization of the vascular endothelium.  $\beta$ -Galactosidase-stained yolk sacs are shown. Scale bars, 1 mm.

## REPORTS

PAR1 deficiency. In both TIE2p/*e-LacZ* mice and TIE2p/*e-PAR1* E9.5 embryos, transgene expression was detected only in endothelium and endocardium and in a small number of circulating cells [Fig. 3A and (19)]. Taken together, our results strongly suggest that the death of *Par1*<sup>-/-</sup> embryos is due to a lack of PAR1 in endothelial cells.

Is thrombin the endogenous activator of endothelial PAR1 during embryonic development, and is PAR1 the major effector of the coagulation cascade in this setting? There are similarities between the phenotypes of *Par1*<sup>-/-</sup> embryos and coagulation factor knockout embryos. Most of tissue factor-deficient embryos (85 to 100%) die at mid-gestation with yolk sac vascular defects (6) and bleeding (5, 7). These observations suggested that tissue factor might contribute to blood vessel development and/or hemostasis in the embryo via its ability to activate the coagulation cascade, by direct signaling or, by other unknown mechanisms (5–7). About 50% of embryos deficient in factor V (*FV*<sup>-/-</sup>), a cofactor necessary for thrombin production, die between E9.5 and E10.5 with multiple abnormalities, including hemorrhage (8). Likewise, ~50% of prothrombin-deficient embryos die between E9.5 and E11.5; bleeding was described in one report (9) but not in another (10). Whether the decreased penetrance of the prothrombin and factor V versus the tissue factor phenotype is due to maternal coagulation factors reaching the embryonic circulation or to a thrombin-independent role for tissue factor is unknown. The similar phenotypes of *Par1*<sup>-/-</sup>, *FV*<sup>-/-</sup>, and prothrombin-deficient embryos suggested a simple model in which factor V mediates conversion of prothrombin to thrombin that then signals via PAR1 (Fig. 4A). If this model were true, the phenotype resulting from combined deficiency of PAR1 and factor V should be identical to that of either deficiency alone. This was not the case. Comparison of embryos deficient in PAR1 or factor V to those lacking both genes revealed synthetic lethality (Fig. 4B). Only 4% (1/23) of *FV*<sup>-/-</sup> *Par1*<sup>-/-</sup> embryos survived to E12.5, a rate markedly less than that of either *Par1*<sup>-/-</sup> or *FV*<sup>-/-</sup> embryos (52% or 67% at E12.5, respectively) and significantly less than the 35% survival rate predicted if PAR1 and factor V deficiencies caused death independently. The 22 dead *FV*<sup>-/-</sup> *Par1*<sup>-/-</sup> embryos were pale, runted, and severely necrotic with pericardial effusions and blood pooled in their pericardial and exocoelomic cavities. Of note, this phenotype and degree of lethality is similar to that reported for the tissue factor-knockout mouse (5–7). The synthetic lethality of combined factor V and PAR1 deficiency suggests that the factor V and PAR1 pathways interact and raises intriguing possibilities. The observation that PAR1 deficiency

enhanced death of *FV*<sup>-/-</sup> embryos suggests that PAR1 can be activated in the absence of embryonic factor V. Thus, molecules other than factor V might mediate activation of prothrombin and/or molecules other than thrombin might mediate activation of PAR1 during development (Fig. 4C). We cannot conclude this rigorously because factor V from the *FV*<sup>+/-</sup> mothers [used by necessity in these experiments (8)] may enter *FV*<sup>-/-</sup> embryos and support some thrombin signaling via PAR1. Loss of such signaling would explain how PAR1 deficiency exacerbates the phenotype of *FV*<sup>-/-</sup> embryos. Looking at the data from another perspective, the observation that factor V deficiency enhanced death of *Par1*<sup>-/-</sup> embryos clearly implies that factor V has actions beyond activating PAR1 during development (Fig. 4C). Our observations

suggest that thrombin and/or another factor V-dependent agonist act on PAR1 and on other target(s) with interacting functions during embryonic development.

Fibrinogen was one potential other target. Although not necessary for development in otherwise normal embryos (20), fibrinogen might become important in the context of the bleeding diathesis seen in *Par1*<sup>-/-</sup> embryos. However, in a study analogous to that in Fig. 4B, fibrinogen deficiency did not enhance death of *Par1*<sup>-/-</sup> embryos at E12.5. It is possible that fibrinogen from the *Fib*<sup>+/-</sup> mothers [used by necessity in these studies (20)] entered the embryonic circulation in sufficient quantity to prevent a phenotype, but, at face value, this negative result suggests that still other coagulation protease substrates are important for embryonic development. Other

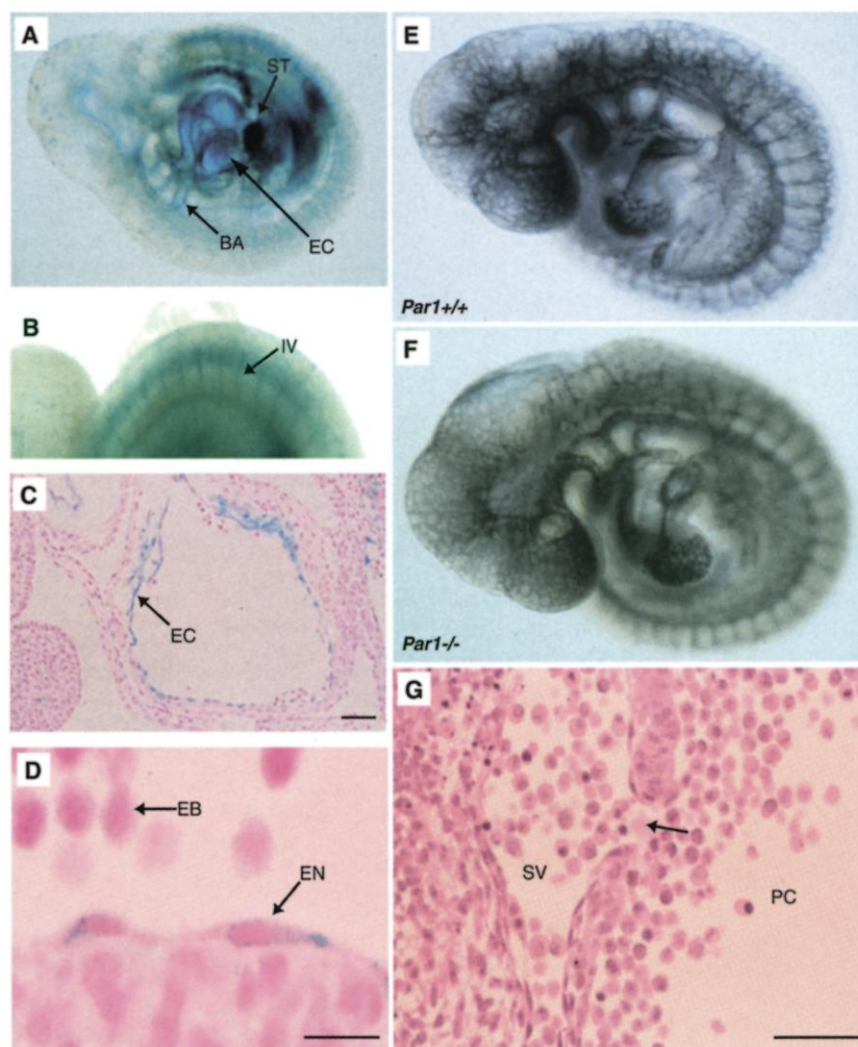


**Fig. 2.** PAR1 expression and *Par1*<sup>-/-</sup> vessels at E9.5. (A to D)  $\beta$ -Galactosidase stain of unaffected homozygous PAR1-*LacZ* knock-in embryos. (A and B) Whole-mount  $\beta$ -galactosidase staining. BA, branchial arch; EC, endocardium; ST, septum transversum; IV, intersomitic vessel. (C and D) Histological sections. Note staining of endocardium (EC) and endothelium (EN) of great vessels. EB, embryonic blood. (E and F) PECAM-1 staining of wild-type (E) and *Par1*<sup>-/-</sup> (F) embryos. (G) Section from a *Par1*<sup>-/-</sup> embryo like that in Fig. 1D showing a defect (arrow) in the wall of the sinus venosus (SV) large enough to allow blood cells into the pericardial cavity (PC). Scale bars, 50  $\mu$ m in (C) and (G); 12  $\mu$ m in (D).

REPORTS

PARs are appealing candidates. Indeed, the notion that other PARs might in part compensate for PAR1 deficiency offers one explanation for both the partiality of the PAR1 phenotype and the synthetic lethality seen with PAR1 and factor V deficiencies. This hypothesis can be tested by using mice with multiple PAR deficiencies.

Our results show that PAR1 function in endothelium and/or endocardium contributes to mouse embryonic development and highlight a role for the coagulation system in directly regulating endothelial cell function during blood-vessel formation. Loss of PAR1 signaling in endothelial cells probably ex-

plains, at least in part, death at midgestation caused by knockout of tissue factor (5–7), factor V (8), and prothrombin (9, 10). Bleeding in *Par1*<sup>-/-</sup> embryos might reflect a role for the coagulation cascade and endothelial PAR1 in sensing occasional “spontaneous” breaks in developing blood vessels and mounting an acute hemostatic response. Because platelets are not present at midgestation and because fibrinogen deficiency did not exacerbate bleeding in *Par1*<sup>-/-</sup> embryos, this model raises the possibility of an endothelial-dependent, platelet- and fibrinogen-independent mechanism for effecting hemostatic responses and deserves further exploration. Our

results are equally consistent with models in which the coagulation cascade and endothelial PAR1 signaling contribute to vascular development and integrity in ways unrelated to acute hemostatic responses. The coagulation cascade and PARs may allow nascent vessels to sense permeability to plasma proteins or allow endothelial and/or endocardial cells to monitor their connection to the circulation; roles in regulation of vascular remodeling and/or endothelial-mesenchymal transformation are easily imagined. In addition, ischemia can increase endothelial permeability and can induce parenchymal tissue factor expression in the adult (21), raising the possibility that the coagulation cascade and PARs might provide one means for developing vessels to sense and respond to inadequate tissue perfusion. In culture, thrombin causes cultured endothelial cells to change shape, disrupts cell-cell junctions (22), and increases the permeability of endothelial cell monolayers (23). Thrombin also enhances endothelial responsiveness to vascular endothelial growth factor (24) and fibroblast growth factor (25) and triggers secretion of extracellular matrix proteins (26) and other growth factors such as platelet-derived growth factor (27). Thus PAR1 activation might contribute to vascular development by regulating endothelial cell shape, migration, proliferation, and/or interactions with perivascular cells and extracellular matrix.

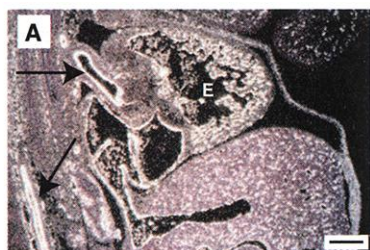
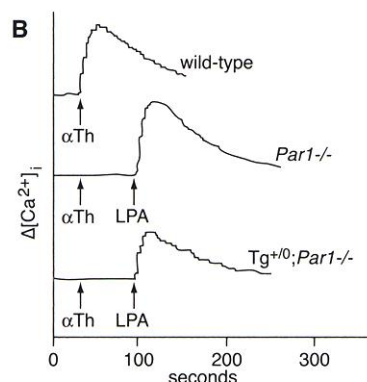


**Fig. 3.** Endothelial expression of PAR1 rescues *Par1*<sup>-/-</sup> animals from death. (A) In situ hybridization for the expression of the TIE2p/e-PAR1 transgene in an E13.5 hemizygous (*Tg*<sup>+ / 0</sup>) embryo using probe to an SV40 sequence tag (12). Dark-field photomicrograph; scale bar, 250  $\mu$ m. Note silver grains indicating expression of the transgene overlying endocardium (E) and endothelium of the great vessels (arrows). Similar results were obtained at E9.5. (B) Cytosolic calcium transients in fibroblasts from wild-type, *Par1*<sup>-/-</sup>, and *Tg*<sup>+ / 0</sup>;*Par1*<sup>-/-</sup> mice were measured using the calcium-sensitive fluor Fura-2. Thrombin ( $\alpha$ Th; 30 nM) or lysophosphatidic acid (LPA; 5  $\mu$ M) were added at the indicated times. (C) Genotypes of offspring alive at weaning from *Tg*<sup>+ / 0</sup>;*Par1*<sup>-/-</sup>  $\times$  *Par1*<sup>+ / -</sup> and *Tg*<sup>+ / 0</sup>;*Par1*<sup>+ / -</sup>  $\times$  *Par1*<sup>-/-</sup> matings. (D) *Par1*<sup>-/-</sup> females were mated with *Tg*<sup>+ / 0</sup>;*Par1*<sup>+ / -</sup> males; embryos were scored at E11.5 to E12.5 as dead or alive on the basis of the absence or presence of a heartbeat, then genotyped by Southern analysis. Five resorbed embryos could not be genotyped and were not included in the analysis; they probably belonged to the *Tg*<sup>0 / 0</sup>;*Par1*<sup>-/-</sup> group.

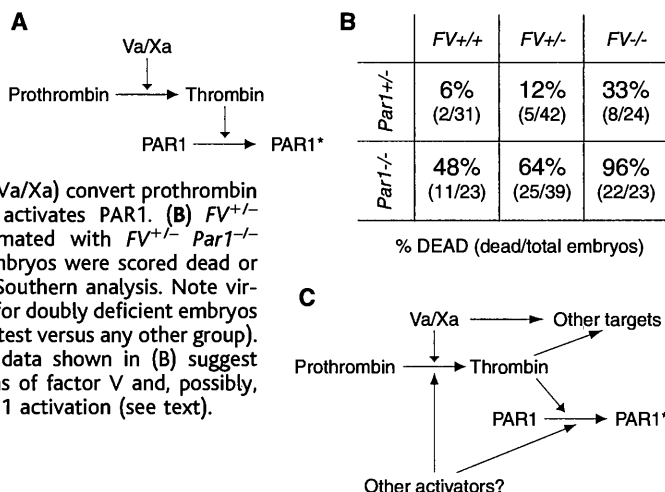


	<i>Par1</i> <sup>+ / -</sup>	<i>Par1</i> <sup>- / -</sup>
<i>Tg</i> <sup>+ / 0</sup>	52	51
<i>Tg</i> <sup>0 / 0</sup>	54	24

	<i>Par1</i> <sup>+ / -</sup>	<i>Par1</i> <sup>- / -</sup>
<i>Tg</i> <sup>+ / 0</sup>	6% (3/48)	14% (5/37)
<i>Tg</i> <sup>0 / 0</sup>	6% (2/33)	39% (11/28)

LIVE OFFSPRING      % DEAD (dead/total embryos)

**Fig. 4.** Interaction of factor V and PAR1 deficiencies. (A) Role of factor V and PAR1 in development: initial model. A simple linear pathway in which activated factors V and X (Va/Xa) convert prothrombin to thrombin that then activates PAR1. (B) *FV*<sup>+ / -</sup>;*Par1*<sup>+ / -</sup> females were mated with *FV*<sup>+ / -</sup>;*Par1*<sup>- / -</sup> males. E11.5 to E12.5 embryos were scored dead or alive and genotyped by Southern analysis. Note virtually complete lethality for doubly deficient embryos ( $P < 0.001$  by chi-square test versus any other group). (C) Revised model. The data shown in (B) suggest PAR1-independent actions of factor V and, possibly, alternative routes to PAR1 activation (see text).



References and Notes

1. R. W. Colman, V. J. Marder, E. W. Salzman, J. Hirsh, in *Hemostasis and Thrombosis*, R. W. Colman, V. J. Marder, E. W. Salzman, J. Hirsh, Eds. (Lippincott, Philadelphia, 1994), pp. 3–18.
2. C. T. Esmon, *Blood* **95**, 1113 (2000).
3. S. R. Coughlin, *Nature* **407**, 258 (2000).
4. A. J. Connolly, H. Ishihara, M. L. Kahn, R. V. Farese Jr., S. R. Coughlin, *Nature* **381**, 516 (1996).
5. T. H. Bugge et al., *Proc. Natl. Acad. Sci. U.S.A.* **93**, 6258 (1996).
6. P. Carmeliet et al., *Nature* **383**, 73 (1996).
7. J. R. Toomey, K. E. Kratzer, N. M. Lasky, J. J. Stanton, G. J. Broze Jr., *Blood* **88**, 1583 (1996).
8. J. Cui, K. S. O’Shea, A. Purkayastha, T. L. Saunders, D. Ginsburg, *Nature* **384**, 66 (1996).
9. W. Y. Sun et al., *Proc. Natl. Acad. Sci. U.S.A.* **95**, 7597 (1998).
10. J. Xue et al., *Proc. Natl. Acad. Sci. U.S.A.* **95**, 7603 (1998).
11. A. L. Darrow et al., *Thromb. Haemost.* **76**, 860 (1996).
12. Mice and analyses. *Par1*<sup>-/-</sup> (4), *FV*<sup>+ / -</sup> (8), and *Fib*<sup>+ / -</sup> (20) mice that had been backcrossed into the C57BL/6J background (>97%) were used. TIE2p/e-LacZ (19) transgenic mice were bred with *Par1*<sup>-/-</sup> mice. To generate precisely timed pregnancies for Fig. 1, matings were restricted to a 1-hour interval (8 a.m. to 9 a.m.) with 9 a.m. counted as E0. In other cases, matings were set up overnight, and females were checked for vaginal plugs each morning before 10 a.m. Noon on the day of plug detection was counted as E0.5. Genotypes were assessed by Southern blot analysis of genomic DNA from embryonic or yolk sac tissue as described in supplementary material (28). To analyze embryos for microscopic bleeding, pregnant mice were killed and perfusion-fixed with 4% paraformaldehyde. To avoid artifacts related to dissection, whole gravid uterine segments were then removed en bloc, immersion-fixed overnight, dehydrated,

# UDP–Glucose Dehydrogenase Required for Cardiac Valve Formation in Zebrafish

Emily C. Walsh and Didier Y. R. Stainier\*

Cardiac valve formation is a complex process that involves cell signaling events between the myocardial and endocardial layers of the heart across an elaborate extracellular matrix. These signals lead to marked morphogenetic movements and transdifferentiation of the endocardial cells at chamber boundaries. Here we identify the genetic defect in zebrafish *jekyll* mutants, which are deficient in the initiation of heart valve formation. The *jekyll* mutation disrupts a homolog of *Drosophila* Sugarless, a uridine 5'-diphosphate (UDP)–glucose dehydrogenase required for heparan sulfate, chondroitin sulfate, and hyaluronic acid production. The atrioventricular border cells do not differentiate from their neighbors in *jekyll* mutants, suggesting that *Jekyll* is required in a cell signaling event that establishes a boundary between the atrium and ventricle.

Cardiac valves form at chamber boundaries and function to prevent retrograde blood flow through the heart. Extensive work in a chick explant system has revealed some of the cellular interactions necessary for valve formation (1). Endocardial cells at the boundary between the atrium and ventricle are prepartened to receive a signal from the overlying myocardial cells. This myocardial signal induces the endocardial cells to undergo an epithelial-to-mesenchymal transition, thereby initiating the formation of prevalvular cushions that are later remodeled to form the valves proper. Recent work has implicated transforming growth factor- $\beta$  family members in the myocardial-to-endocardial signaling event that induces endocardial cushion formation (2–5). However, the mechanism by which myocardial cells at the atrioventricular (AV) boundary acquire the competence to send that signal is not known.

Large-scale screens in zebrafish have identified several mutations that affect cardiac valve formation, the most severe of which is the recessive mutation *jekyll* (6). *jekyll* mutant embryos exhibit pericardial edema and toggling of blood between the two chambers of the heart (compare Fig. 1, A and B). Together these phenotypes are generally indicative of defective AV valve function and are consistent with previous observations that *jekyll* mutant hearts lack valve tissue at 48 hours postfertilization (hpf) (6). To analyze endocardial morphology in vivo, we generated a line of *jekyll* heterozygotes bearing an integrated mouse *tie2* promoter driving green fluorescent protein (GFP) expression in the

developing endocardium (7). In wild-type embryos, endocardial cells cluster at the AV boundary at the onset of valve formation at 43 hpf (Fig. 1C). However, in mutant hearts this clustering fails to occur (Fig. 1D), indicating that *jekyll* function is required for this early endocardial morphogenetic event.

To gain further insight into the *jekyll* valve defect, we isolated the disrupted gene by synteny cloning. We localized *jekyll* to a centromeric region of linkage group 1 using bulk segregant analysis (8) of embryos genotyped for polymorphic CA repeat markers. We then performed fine mapping of the region with 15 polymorphic markers on 200 wild-type haploid embryos and found close linkage between *jekyll* and three of these markers. Next, we genotyped an additional 1150 affected diploid embryos with those three markers as well as for a polymorphism in the 3'-untranslated region of *ldb3* (9). These studies allowed us to further narrow the *jekyll* interval to a 0.5-centimorgan region (Fig. 2A).

Examination of the emerging map of the *jekyll* region revealed a striking conservation of synteny with a region of human chromosome 4p. Taking advantage of this conserved synteny, we mapped four zebrafish expressed sequence tags (ESTs) with sequence similarity to human genes in this 4p region. One of these ESTs, corresponding to a homolog of the *sugarless* gene (known as UDP–glucose dehydrogenase in humans and by convention, referred to as *ugdh* hereafter), was found by radiation hybrid mapping to lie between two markers closely flanking the *jekyll* locus. Sequence analysis of cDNA prepared from wild-type and mutant embryos revealed a T to A change at base pair 992 in the mutant allele. Genotyping for this change revealed no recombination between *jekyll* and the observed lesion in 2870 meioses (Fig. 2, A and B) (10). The T to A change results in an

embedded in paraffin, sectioned (10  $\mu$ m), and stained with hematoxylin and eosin. Whole-mount  $\beta$ -galactosidase staining and immunostaining for PECAM-1 (29) and in situ hybridization for PAR1 mRNA (77) and for an SV40 sequence tag in the TIE2p/e-PAR1 transgene mRNA (30) were performed as described.

13. S. Offermanns, C. F. Toombs, Y. H. Hu, M. I. Simon, *Nature* **389**, 183 (1997).
14. G. R. Sambrano, E. J. Weiss, Y. W. Zheng, W. Huang, S. R. Coughlin, *Nature*, in press.
15. R. A. Shivdasani et al., *Cell* **81**, 695 (1995).
16. R. Rugh, *The Mouse: Its Reproduction and Development* (Oxford Univ. Press, New York, 1990).
17. S. J. Soifer, K. G. Peters, J. O'Keefe, S. R. Coughlin, *Am. J. Pathol.* **144**, 60 (1994).
18. Constructs. In the PAR1-LacZ knock-in targeting vector, the start ATG and codons 2 to 4 of PAR1 exon 1 were replaced with a LacZ-PGK-Neo<sup>R</sup> cassette. A Kozak sequence immediately preceded the LacZ gene. A 1320–base pair (bp) short arm 5' of the LacZ-PGK-Neo<sup>R</sup> cassette, a 4.5-kb long arm 3' of the LacZ-PGK-Neo<sup>R</sup> cassette, and a 509-bp Southern probe 5' of the short arm (i.e., outside of the targeting construct) were generated by PCR of BAC DNA containing the PAR1 gene. Primers and Southern analysis were as described in supplementary material (28). The Neo<sup>R</sup> cassette was in the same transcriptional direction as PAR1 and was bounded by loxP sites. In vivo cre-mediated excision of the Neo<sup>R</sup> cassette using  $\beta$ -actin-cre transgenic mice decreased the intensity of  $\beta$ -galactosidase staining but did not change the overall pattern. For the TIE2p/e-PAR1 transgenic construct a 1.2-kb Eco RI/Xba I (blunted) fragment containing the PAR1 cDNA coding region was inserted 5' to an 847-bp fragment of SV40 small t intron and poly(A) sequence from the vector CPV2 (30) in pBluescript SK (Stratagene). A 2.1-kb Hind III fragment containing the TIE2 promoter and a 9-kb fragment containing the TIE2 enhancer from pHHNS (19) were inserted 5' and 3' to the 2-kb PAR1-SV40, respectively. The resulting 13.1-kb insert was used for microinjections.
19. T. M. Schlaeger et al., *Proc. Natl. Acad. Sci. U.S.A.* **94**, 3058 (1997).
20. T. T. Suh et al., *Genes Dev.* **9**, 2020 (1995).
21. J. H. Erlich et al., *Am. J. Pathol.* **157**, 1849 (2000).
22. M. J. Rabiet et al., *Arterioscler. Thromb. Vasc. Biol.* **16**, 488 (1996).
23. V. Vouret-Craviari, P. Boquet, J. Pouyssegur, E. Van Obberghen-Schilling, *Mol. Biol. Cell* **9**, 2639 (1998).
24. N. E. Tsopanoglou, M. E. Maragoudakis, *J. Biol. Chem.* **274**, 23969 (1999).
25. D. Gospodarowicz, K. D. Brown, C. R. Birdwell, B. R. Zetter, *J. Cell Biol.* **77**, 774 (1978).
26. E. Papadimitriou et al., *Am. J. Physiol.* **272**, C1112 (1997).
27. T. O. Daniel, V. C. Gibbs, D. F. Milfay, M. R. Garovoy, L. T. Williams, *J. Biol. Chem.* **261**, 9579 (1986).
28. Supplementary material is available on Science Online at [www.sciencemag.org/cgi/content/full/293/5535/1666/DC1](http://www.sciencemag.org/cgi/content/full/293/5535/1666/DC1)
29. T. M. Schlaeger, Y. Qin, Y. Fujiwara, J. Magram, T. N. Sato, *Development* **121**, 1089 (1995).
30. Y. Srinivasan, F. J. Lovicu, P. A. Overbeek, *J. Clin. Invest.* **101**, 625 (1998).
31. We thank D. Ginsburg of University of Michigan, Ann Arbor, for *FV<sup>+/-</sup>* mice, J. Degen of Children's Hospital, Cincinnati, for *Fib<sup>+/-</sup>* mice, T. Sato of University of Texas, Southwestern, for TIE2p/e-LacZ transgenic mice and pHHNS DNA, and G. Martin and B. Black of UCSF for  $\beta$ -actin-cre and smooth muscle  $\alpha$ -actin promoter-LacZ transgenic mice, respectively; R. Hamilton and J. Wong for the electron microscopy studies; L. Prentice and R. Advincula for technical assistance; G. Martin, H. Bourne, I. Herskowitz, D. Stainier, and P.-T. Chuang of UCSF for critical reading of this manuscript. C.T.G. was supported by a predoctoral fellowship from the American Heart Association, Western States Affiliate. This work was supported in part by NIH HL44907 and HL65590.

Department of Biochemistry and Biophysics, Programs in Developmental Biology, Genetics and Human Genetics, University of California, San Francisco, CA 94143–0448, USA.

\*To whom correspondence should be addressed. E-mail: [didier\\_stainier@biochem.ucsf.edu](mailto:didier_stainier@biochem.ucsf.edu)

2 April 2001; accepted 2 July 2001